Date of publication JUN-30, 2024, date of current version FEB-09, 2024.
www.computingonline.net / computing@computingonline.net

Print ISSN 1727-6209
Online ISSN 2312-5381
DOI 10.47839/ijc.23.2.3537

Full Diversity Space Time Codes for Next Generation Wireless Sensor Networks

MOHAMED S. ABOUZEID, HEBA A. EL-KHOBBY, MAHMOUD A. A. ALI, MOHAMED E. NASR
Electronics and Electrical Communication Engineering Department, Faculty of Engineering,
Tanta University, Tanta 31733, Egypt

Corresponding author: Mohamed S. Abouzeid (e-mail: mohamed.sayed@f-eng.tanta.edu.eg).

ABSTRACT For the next generation of wireless sensor networks, this research paper proposes two distinguished, robust space-time codes with low complexity and full diversity. The channel is constructed using Quasi-deterministic radio channel generation (Quadriga), which pursues a geometric stochastic model. This paper discusses an uplink perspective on an industrial communication system. A master node design with four distributed antennas is suggested. Two antennas are available on slave nodes, where the proposed space time coding can be used. Additionally, zero-forcing (ZF) and minimum mean squared error (MMSE)-based low-complexity decoders are designed. The proposed codes outperform the Alamouti code under identical circumstances, according to simulation data. The simulation results show that a coding gain of about 5dB in comparison to Alamouti code is achieved. A high coding gain is attained, which results in a more reliable transmission, according to the bit error rate (BER). This research paper significantly contributes to the standardization of the next-generation wireless sensor networks.

KEYWORDS Space Time Code (STC); Zero Forcing Algorithm (ZF); Minimum Mean Squared Error Detector (MMSE); Quadriga; Wireless Sensor Network (WSN).

I. INTRODUCTION

TODAY, a variety of industries are boosting the efficiency of their operating processes in response to rising demand. A research area in the next-generation wireless sensor networks (WSNs) is industrial communication. Increasing the operational effectiveness of industrial control processes is one of the important needs for industrial communication systems [1]. Reduced capital expenditures should also be used to support more adaptable operations [2-4]. Recently, the use of wireless communication technology in industrial applications, most notably in Wireless Sensor Networks (WSN), has attracted a lot more interest [3]. It is anticipated that industrial wireless communication will be able to give processes a high level of real-time dynamic control [5]. The benefits of wireless technologies, such as their retrofitability and intrinsic flexibility, also present a significant opportunity for the development of industrial communication in the future [6, 7].

The state-of-the-art wireless technology, however, was unable to handle the demanding communication robustness required by the industrial environment's extreme channel conditions [8, 9]. In industrial settings, there are metal structures for pumps, robots, pipes, and other devices [10]. High scattering is therefore a fundamental element in industrial contexts [11]. The salve nodes can also be protected by metal structures in a given direction at a specific time [12]. The performance as a result is dramatically worsened [13].

MIMO approaches may be the best option for achieving high dependability through spatial diversity [14]. Space-time code, in particular, can be used to good effect to harness the spatial diversity produced by multiple signal transmissions [15, 16]. The space-time code with coding gain and diversity order offers the best solution for meeting the reliability requirements of the next-generation wireless sensor networks.

Youn et al. [17] proposed a cooperative space-time line code (C-STLC) technique for a relay-assisted Internet of Things (R-IoT) in which each relay IoT device (RID) sends the STLC encoded signal to a single access point (AP) at the second hop after successfully decoding the signal received from a source IoT device at the first hop. In addition to being intricate in nature, this operation takes a long time. The authors of [18] suggested a framework that uses space spreading in conjunction with either {time or frequency diversity, or both} to lessen interference and signal loss caused by channel impairments and to enable the effective functioning of densely populated, large-scale Internet of Things (IoT). Thus, this reduced the chance of the transmission side interference. Using array-processing gain, a multiple-antenna array on the receiving side improved performance in the presence of channel impairments. The drawback of this technology is that only one device may communicate at a time; two devices cannot transmit on the same block.

Rajawat et al. [19] demonstrated how Reinforcement Learning (RL) can help make industrial production systems resilient and adaptable so they can react to changes instantly. The application of RL in a variety of adaptive cognitive systems with Industrial IoT-edges in manufacturing processes was investigated in this work. Nonetheless, a lot of events in Industrial IoT applications need for real-time decision processing. These occurrences are frequently extremely scant and complicated and often without enough information to make conclusions. The array concept presented by the authors in [20] is made up of tiny, spatially dispersed subarrays that can fit inside the non-metallic components of an automobile. In order to compensate for the delays, space-time adaptive processing was added. Nevertheless, the Space-Time Adaptive Processing (STAP) was limited in its performance by the number of taps examined in a simulation with various fractional delays.

The distributed antenna system (DAS) increases spectrum efficiency while also improving energy efficiency [21, 22]. The antennas in a distributed antenna system are scattered throughout the service area and connected to a centralized core node known as a master node (MN) [23, 24]. The received signal's quality is greatly enhanced by this structure. On the basis of channel state information (CSI), recent research has shown the potential of DAS [25-27]. To the best of the authors' knowledge, no research projects have examined the performance of a distributed antenna system coupled with space-time coding in a next-generation wireless sensor network (WSN). This research area is of great concern for the standardization of next-generation wireless sensor networks.

Two space-time codes are presented in this research for the use in the next-generation wireless sensor networks. From an uplink (UL) standpoint, the system configuration for WSN is addressed. The sensor network is covered by a consistent distribution of MN antennas. As a result, slave nodes and MN can have a line of sight (LoS). In order to use the proposed space-time coding, it is presumed that the slave nodes have two antennas. In order to construct a highly dependable WSN, a new space-time code is formulated. Additionally, the decoding process is carried out by low-complexity linear decoders designed using the Minimum Mean Squared Error (MMSE) and Zero Forcing (ZF) algorithms. In comparison to existing STC systems, a low-complexity space-time code can be developed. The effectiveness of the proposed space-time coding schemes in improving the dependability of the next-generation WSNs and communication quality will be examined in contrast to the commonly used Alamouti code in terms of BER.

The rest of the paper is organized as follows. The system model is described in Section II. In Section III, channel modelling for industrial wireless systems is developed. A signal representation for Section IV is formulated. In Section V, the proposed coding systems are presented. Section VI demonstrates simulation results. Section VII provides a conclusion.

II. MODELLING OF THE SYSTEM

The proposed uplink system model for a sensor network with a (50 m x 50 m) spatial dimension is made clear in Figure 1.

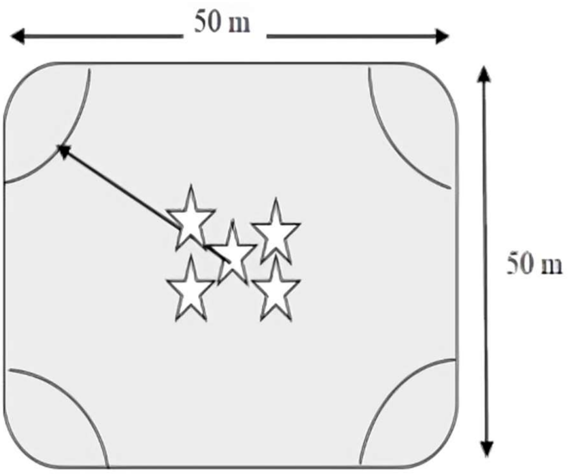

Figure 1. WSN system model

Over the network region, the slave nodes are uniformly and properly distributed. The MN is linked to distributed antennas so that they are precisely synchronized with one another and connected to a high-speed, larger-capacity link. This work makes the assumption that the proposed space-time codes can be used in SNs with two antennas. Each node is about $25\sqrt{2}$ m away from the distribution of antennas thanks to the collocation of SNs in the network's core. It is expected that there are N_m total MN antennas with K SNs.

III. INDUSTRIAL WSN CHANNEL MODELLING

The wireless channel in industrial WSNs has a distinct statistical analysis from the free-space urban region. Concrete walls and metal ceilings are common in industrial automation [28]. There is considerable multipath as a result. In this paper, the Quadriga channel formulation has been applied for realistic results and estimating the accurate performance of industrial WSN [29, 30]. Quadriga develops a geometric stochastic channel model that it uses to produce the channel parameters [30].

Numerous multipath components that are supplemented by the dispersed sensor network represent each channel. At the carrier frequency f_c, the channel impulse response between the m^{th} transmit antenna and the k^{th} receive antenna is expressed as [31].

$$g_{km}^{n}(t)=\sum_{c=1}^{p_T}\sqrt{p_c}.e^{j\theta_c}.\delta_c(t-\tau_c)\,, \tag{1}$$

where P_c, θ_c and τ_c are the c^{th} path received power, phase angle, and time delay, respectively. δ_c is the delta impulse function, and P_T represents the total number of paths. Calculations for the frequency response at the carrier frequency f_c between the m^{th} transmit antenna and the k^{th} receive antenna are given in [32].

$$h_{km}^{n}=\sum_{c=1}^{P_T}\sqrt{P_c}.e^{J\theta_c}.e^{j2\pi f_c\tau_c}\,, \tag{2}$$

where f_c is the carrier frequency. The carrier frequency used in this research is 5.8 GHz, which is the standard frequency used in industrial applications [33].

The channel coefficients between the K^th transmit antenna and the m^th receive antenna are denoted by H_i, where $H_i = \frac{1}{(d_i/d_0)^{\alpha/2}} h_{km}$, α is the path-loss exponent and d_0 is the reference distance. As the path-loss in an obstructed industrial WSN spans from 2 to 3, a path-loss exponent of 2.5 is used in this research [34-36].

IV. SIGNAL REPRESENTATION

This section expresses the proposed space-time code signal representation. Assume that STBC is used to transmit the signal by each Slave Node (SN) in the sensor network. The code of K^{th} SN is expressed as X_k with a size of 2 × T. The received signal by MN in T time slots can be expressed as follows:

$$Y = \sum_{k=1}^{K} \sqrt{\frac{\rho}{2}} H_k X_k + n_k , \quad (3)$$

where $H_k \in \mathbb{C}^{4X2}$ represents the channel fading coefficients from the K^{th} slave node to the master node antennas. $n_k \in \mathbb{C}^{4X2}$ represents zero mean, unit variance complex Gaussian random variables. The entries of the random noise are independent and are identically distributed (i.i.d). ρ represents the received SNR. $\sqrt{\frac{1}{2}}$ is used to normalize the transmitted signal energy to be 1 in each time slot.

V. THE PROPOSED CODING SCHEMES

For next-generation wireless sensor networks, the proposed space-time coding techniques for the transmitted signal from the slave nodes (SN) to the master node (MN) antennas are provided in this section. The transmitted signal at MN is then estimated using a nearly optimal low-complexity linear decoder that is designed. One SN with two transmitting antennas is the case that we are considering. Let X_k be the transmitted signal from the two transmit antennas at SN over two time slots, where $X_k \in \mathbb{C}^{2XT}$. In this research project $T = 2$ is chosen.

A. Proposition STC 1

The suggested space-time code is formulated as follows:

$$X_k = \begin{pmatrix} -as_1 - cs_2 & -ds_2^* + bs_1^* \\ -bs_2^* - ds_1^* & cs_1 + as_2 \end{pmatrix}, \quad (4)$$

where s_1 and s_2 are the transmitted symbols over 2 Time slots leading to achieving a code rate of 1. Here $*$ indicates complex conjugate. Using a QAM constellation, these symbols are developed. Complex valued-design parameters that will be defined later are *a*, *b*, *c*, and *d*.

It is assumed that over the course of the coding block period, the channel coefficients are quasi-static, meaning they are unchanged with regard to time. Thus, the equivalent channel from one slave node to master node can be described by $H_k = [h_{k1} \quad h_{k2}]$.

By substitution, equation (3) can be rewritten as follows:

$$Y = \sum_{k=1}^{K} \sqrt{\frac{\rho}{2}} \tilde{H}_k \tilde{X}_k + \tilde{n}_k , \quad (5)$$

where $\tilde{H}_k = \begin{pmatrix} -ah_{k1} & -ch_{k1} & bh_{k2} & -dh_{k2} \\ ch_{k2} & ah_{k2} & dh_{k1} & bh_{k1} \end{pmatrix}$ and $\tilde{X}_k = [s_1 \quad s_2 \quad -s_2^* \quad s_1^*]$.

The proposed code achieves orthogonality because it meets $XX^H = \alpha I$

$$XX^H = \begin{pmatrix} -as_1 - cs_2 & -ds_2^* + bs_1^* \\ -bs_2^* - ds_1^* & cs_1 + as_2 \end{pmatrix} * \begin{pmatrix} -as_1^* - cs_2^* & -bs_2 - ds_1 \\ -ds_2 + bs_1 & cs_1^* + as_2^* \end{pmatrix} \quad (6)$$

$$= \begin{pmatrix} (-as_1 - cs_2)^2 + (-ds_2 + bs_1)^2 \\ + (-bs_2 - ds_1)^2 + (cs_1 + as_2)^2 \end{pmatrix} \begin{bmatrix} 1 & 0 \\ 0 & 1 \end{bmatrix}$$

The transmission of equal average power for each symbol time is the restriction used to generate this STC such that $|a|^2 + |b|^2 = |c|^2 + |d|^2$. This constraint helps simplify the optimization procedure to determine the parameters *a*, *b*, *c* and *d*.

In equation (4), the proposed space-time code X_k is a maximum likelihood (ML) detectable with an exhaustive search complexity of $O(M^2)$, where M is the constellation size. The exhaustive search examines all potential values of the transmitted symbols (s1, s2) and selects (s1, s2) that minimizes the Euclidean distance D(s1, s2):

$$D(s_1, s_2) = \sum_{k=1}^{N_r} \left| y_{k1} - h_{k1}(-as_1 - cs_2) - h_{k2}(-bs_2^* - ds_1^*) \right|^2 + \sum_{l=1}^{N_r} \left| y_{l2} - h_{l1}(-ds_2^* + bs_1^*) - h_{l2}(cs_1 + as_2) \right|^2 \quad (7)$$

By expanding $D(S_1,S_2)$, equation (7) can be rewritten as follows:

$$D(s_1, s_2) = C + g(s_1, s_2) + \sum_{k=1}^{N_r} 2\Re\{h_{k1}h_{k2}^*(ab^* s_1 s_2 + cd^* s_2 s_1 + cb^* |s_2|^2 + ad^* |s_1|^2)\} + 2\Re\{h_{l1}h_{l2}^*(-dc^* s_2^* s_1^* + ba^* s_1^* s_2^* - da^* |s_2|^2 + bc^* |s_1|^2)\}, \quad (8)$$

where C is a function of the symbol pair and a constant that is independent of the symbols. The following variables have been utilized to minimize the Euclidean distance:

$$\begin{aligned} a &= \frac{1}{\sqrt{2}} + J\frac{1}{\sqrt{2}} \\ b &= 1-\sqrt{7} + J\frac{1+\sqrt{7}}{4\sqrt{2}} \\ c &= 1-\sqrt{7} - J\frac{1+\sqrt{7}}{4\sqrt{2}} \\ d &= \frac{1}{\sqrt{2}} - J\frac{1}{\sqrt{2}} \end{aligned}. \quad (9)$$

B. Proposition STC 2

The other space-time code can be designed as follows:

$$X_k = \begin{pmatrix} as_1 + cs_2 & ds_1^* + bs_2^* \\ -bs_1^* - ds_2^* & cs_1 + as_2 \end{pmatrix}, \quad (10)$$

where s_1 and s_2 are the symbols that were transmitted throughout two time slots to obtain a code rate of 1. Here $*$ indicates complex conjugate. These symbols are produced by the QAM constellation.

Equation (3) can be rewritten as follows under the same circumstances $H_k = [h_{k1} \quad h_{k2}]$, such that

$$Y = \sum_{k=1}^{K} \sqrt{\frac{\rho}{2}} \widehat{H}_k \widehat{X}_k + \widehat{n}_k, \quad (11)$$

where $\widehat{H}_k = \begin{pmatrix} ah_{k1} & ch_{k1} & -bh_{k2} & -dh_{k2} \\ ch_{k2} & ah_{k2} & dh_{k1} & bh_{k1} \end{pmatrix}$ and $\widehat{X}_k = [s_1 \quad s_2 \quad s_1^* \quad s_2^*]$.

The proposed code performs well in achieving orthogonality because it satisfies $XX^H = \alpha \mathrm{I}$

$$XX^H = \begin{pmatrix} as_1 + cs_2 & ds_1^* + bs_2^* \\ -bs_1^* - ds_2^* & cs_1 + as_2 \end{pmatrix} * \begin{pmatrix} as_1^* + cs_2^* & -bs_1 - ds_2 \\ ds_1 + bs_2 & cs_1^* + as_2^* \end{pmatrix} = \begin{pmatrix} (as_1 + cs_2)^2 + (ds_1 + bs_2)^2 + \\ (-bs_1 - ds_2)^2 + (cs_1 + as_2)^2 \end{pmatrix} \begin{bmatrix} 1 & 0 \\ 0 & 1 \end{bmatrix}. \quad (12)$$

The criteria for this STC design are that each symbol transmits the same amount of average total power such that $|a|^2 + |c|^2 = |b|^2 + |d|^2$. This restriction enables us to simplify the optimization process to determine the parameters *a*, *b*, *c*, and *d*.

In equation (10), the proposed space-time code X_k is a maximum likelihood (ML) detectable with an exhaustive search complexity of $O(M^2)$. The exhaustive search determines that the Euclidean distance D (S_1, S_2) should be minimized:

$$\begin{aligned} D(s_1, s_2) &= \sum_{z=1}^{N_r} \left| y_{z1} - h_{z1}(as_1 + cs_2) - h_{z2}(-bs_1^* - ds_2^*) \right|^2 \\ &+ \sum_{t=1}^{N_r} \left| y_{t2} - h_{t1}(ds_1^* + bs_2^*) - h_{t2}(cs_1 + as_2) \right|^2 \end{aligned}. \quad (13)$$

By expanding D (S_1, S_2), equation (13) can be rewritten as follows:

$$\begin{aligned} &D(s_1, s_2) = Q + P(s_1, s_2) + \\ &\sum_{z=1}^{N_r} 2\Re\{h_{z1}h_{z2}^*(-cb^* s_2 s_1 - cd^* s_1 s_2 + cd^* |s_2|^2 - ab^* |s_1|^2)\} \\ &+ 2\Re\{h_{t1}h_{t2}^*(da^* s_1^* s_2^* + bc^* s_1^* s_2^* - ba^* |s_2|^2 + dc^* |s_1|^2)\} \end{aligned}, \quad (14)$$

where Q is a constant independent of the symbols and $P(s_1, s_2)$ is a function of the symbol pair (s_1, s_2). The following parameters have been used to minimize the Euclidean distance.

$$\begin{aligned} a &= 1-\sqrt{7} + J\frac{1+\sqrt{7}}{4\sqrt{2}} \\ b &= \frac{1}{\sqrt{2}} + J\frac{1}{\sqrt{2}} \\ c &= \frac{1}{\sqrt{2}} - J\frac{1}{\sqrt{2}} \\ d &= 1-\sqrt{7} - J\frac{1+\sqrt{7}}{4\sqrt{2}} \end{aligned}. \quad (15)$$

Additionally, to achieve the optimum performance at the receiver side, near-optimal-low complexity zero-forcing (ZF) and minimum mean squared error (MMSE) detectors are designed for decoding the received signal.

Denote

$$\begin{aligned} \bar{H} &= (\tilde{H}_1, \tilde{H}_2, \cdots, \tilde{H}_k) \\ X^t &= (X_1^t, X_2^t, \cdots, X_k^t)^t \end{aligned}$$

Equation (3) can be rewritten as

$$\tilde{Y} = \sum_{k=1}^{K} \sqrt{\frac{\rho}{2}} \bar{H}_k X_k^t + n_k^t. \quad (16)$$

Let us denote

$$\begin{aligned} G_{ZF} &= (\bar{H}^H \bar{H})^{-1} \bar{H}^H \\ G_{MMSE} &= (2I/\rho + \bar{H}^H \bar{H})^{-1} \bar{H}^H, \end{aligned}$$

where G_{ZF} and G_{MMSE} are the matrices of zero forcing and minimum mean squared error algorithms decoder, respectively. The received signal can be estimated by

$$\tilde{X} = G_{MMSE}\tilde{Y}, \tag{17}$$

where $\tilde{X}$ is the estimated received symbols from the slave nodes.

VI. SIMULATION RESULTS

The proposed scenario is depicted in Figure 2 from an uplink perspective. The proposed space-time coding can be used since each slave node (SN) has two antennas. Quadrature phase shift keying (QPSK) is the used modulation. The proposed space-time code formula is implemented using MATLAB simulation platform. For the master node, three cases are investigated. One instance is when the master node (MN) has one antenna. In the second scenario, there are two antennas on the master node (MN). As a result, the performance may be examined using just two antennas dispersed over the sensor network area. MN, which has four distributed antennas, is the other model. The channel parameters are generated stochastically using a quasi-deterministic radio channel generator (Quadriga) [35]. Quadriga uses a stochastic geometry model [36]. Based on statistical distributions extrapolated from several real-time channel measurements, the channel parameters are determined. As a result, it is feasible to get more real accurate results. Quadriga was designed to make it possible to model MIMO radio channels for particular network configurations.

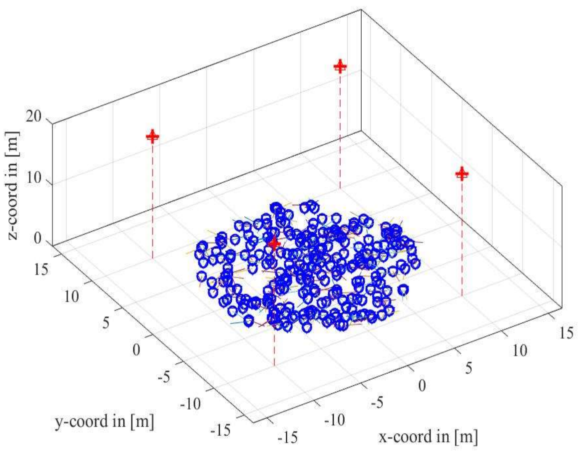

Figure 2. Quadriga model proposed scenario

As shown in Figure 2, the slave nodes represented by the blue circles are distributed randomly within the sensor network region. The master node antennas are placed at the corners of the network region.

For sake of clarification, we present the channel parameters of a WINNER indoor hotspot for typical indoor deployments and the channel parameters of industrial WSN indoor deployments. We compare the K-factor, shadow fading, delay spread and angular spread calculated from the channel coefficients obtained from the measurements and the channel builder from Quadriga.

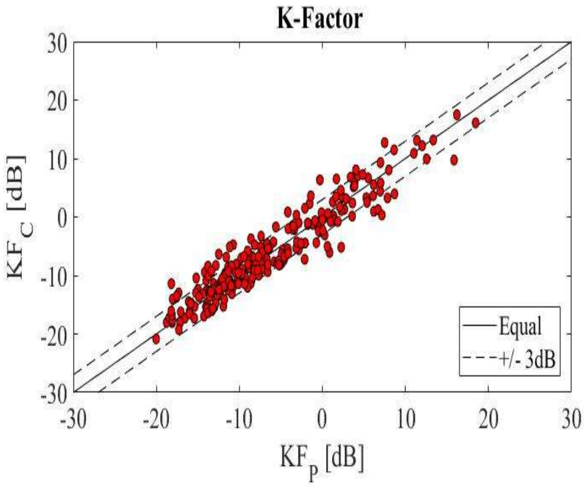

Figure 3. K-factor for industrial indoor deployments

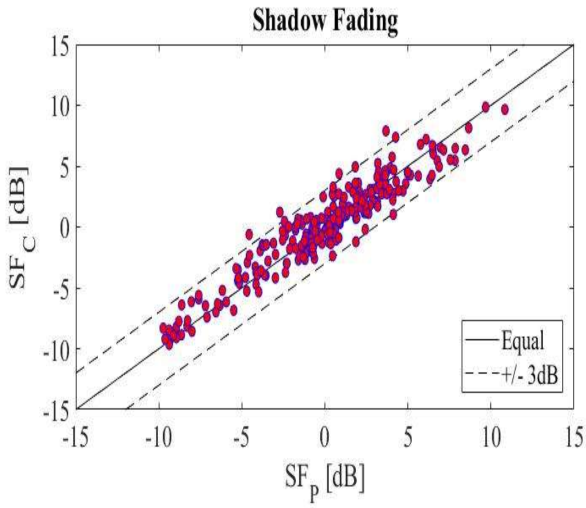

Figure 4. Shadow fading for industrial indoor deployments

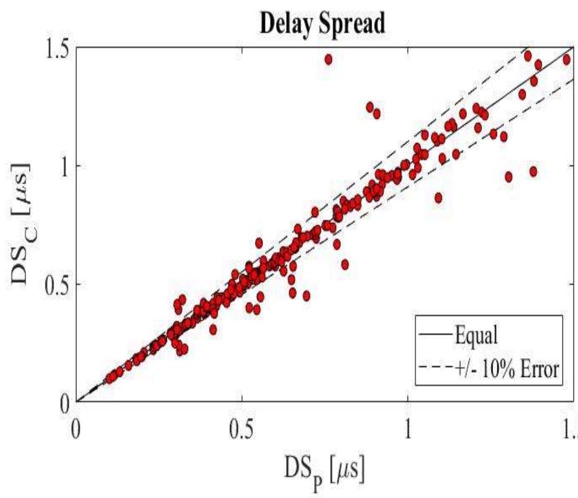

Figure 5. Delay spread for industrial indoor deployments

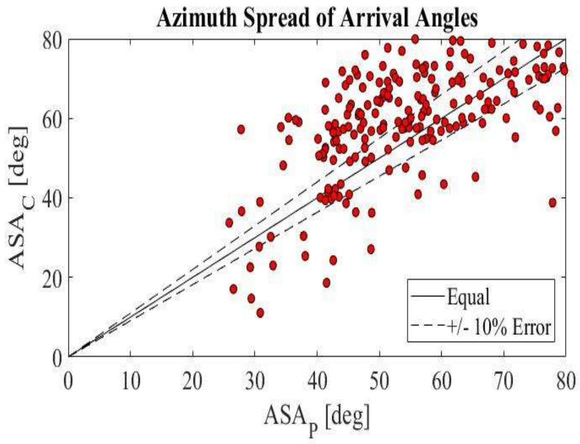

Figure 6. Azimuth spread of arrival angles for industrial indoor deployments

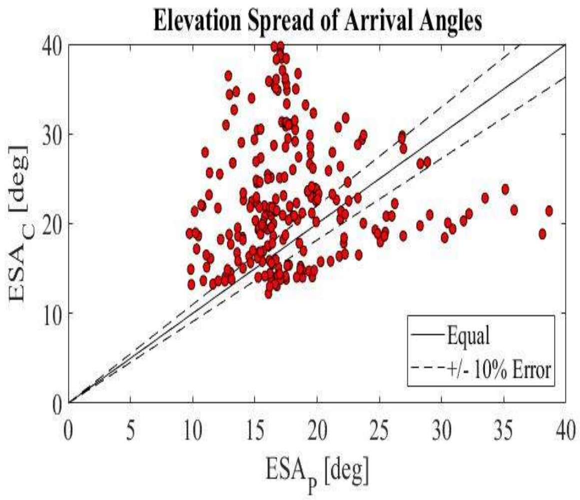

Figure 7. Elevation spread of arrival angles for industrial indoor deployments

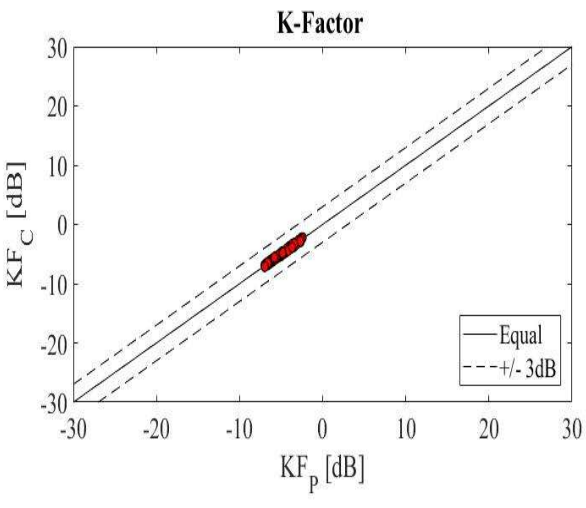

Figure 8. K-factor for typical indoor deployments

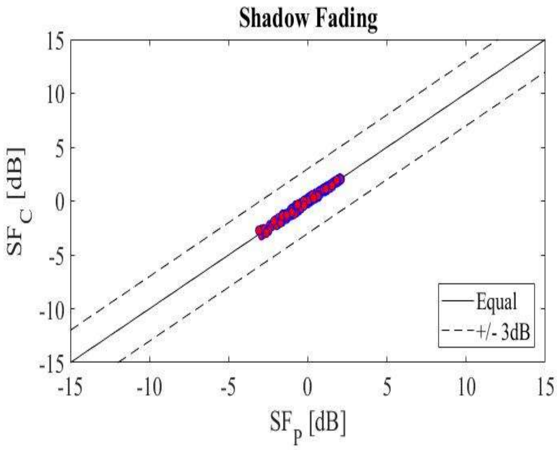

Figure 9. Shadow fading for typical indoor deployments

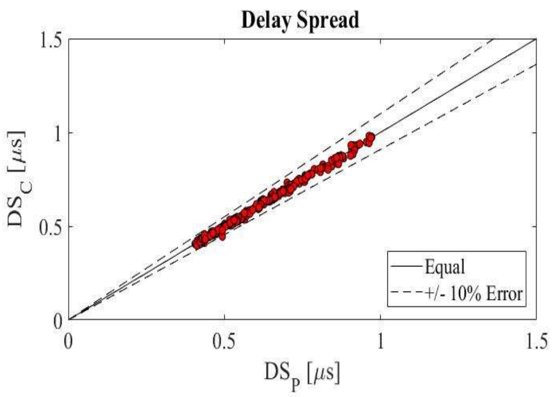

Figure 10. Delay spread for typical indoor deployments

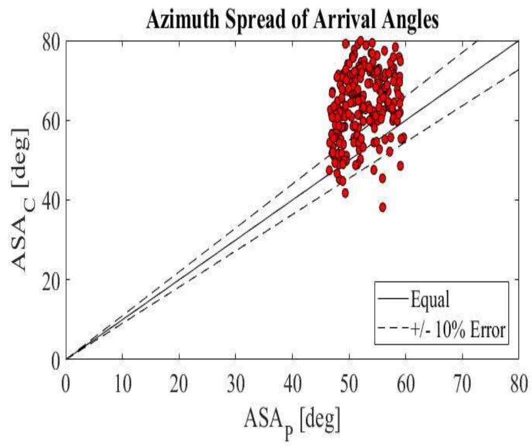

Figure 11. Azimuth spread of arrival angles for typical indoor deployments

As we can in these figures, industrial WSN indoor deployment is a highly scattered environment which limits the performance of wireless communication systems.

Due to its widespread use in numerous wireless communication networks, the Alamouti code is used as a basis to measure the performance of the proposed codes. Firstly, we consider the case of one antenna MN as shown in Figure 12. As we can see in Figure 13, the proposed codes significantly perform better than the Alamouti code. For instance, the coding gain of Proposition 2 is about 5 dB higher than that of Alamouti under the same conditions.

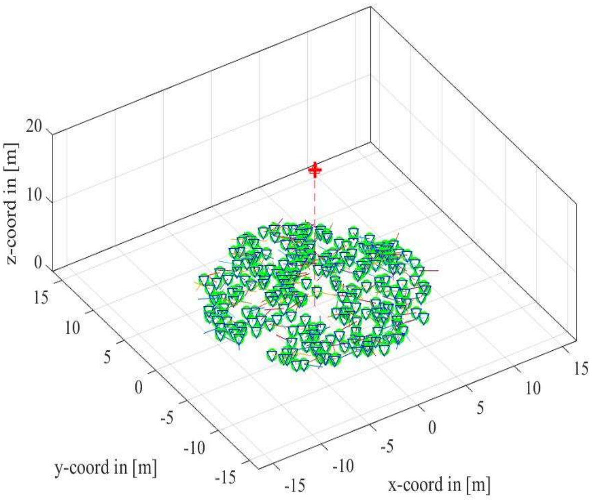

Figure 12. Proposed scenario with one antenna MN

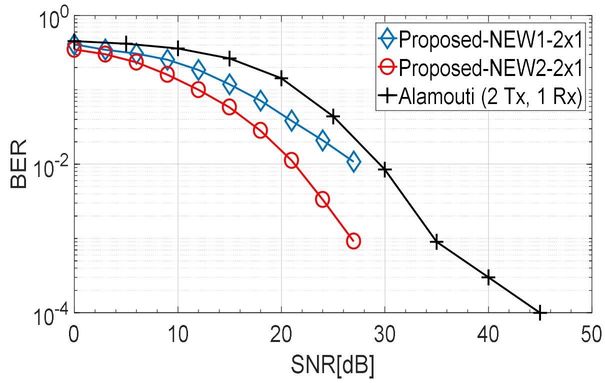

Figure 13. BER performance for the proposed codes and Alamouti code for MN antenna

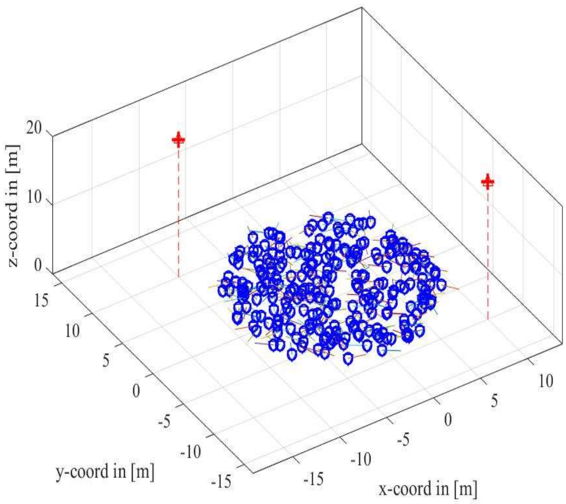

Figure 14. Proposed system for two antennas at the MN

Figure 14 depicts the suggested system for the master node with just two antennas. Figure 15 illustrates how the proposed space-time codes work better than the Alamouti code in the scenario of two transmit antennas at the SN. At low SNR, the proposed space-time code of Proposition 1 outperforms the Alamouti code. However, because of intense scattering and interference, performance suffers at high SNR. As can be observed, the space-time code in Proposition 2 has a coding gain of around 7 dB at BER=10^{-3}. The distribution of antennas and the carefully designed coding parameters are attributable to this.

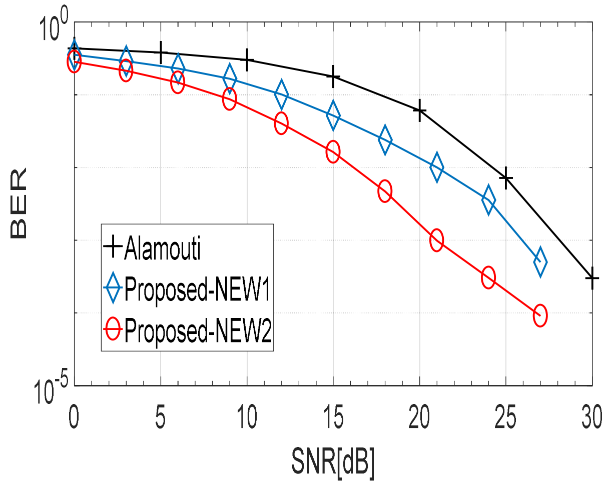

Figure 15. BER performance for the proposed codes and Alamouti code for MN with two antennas

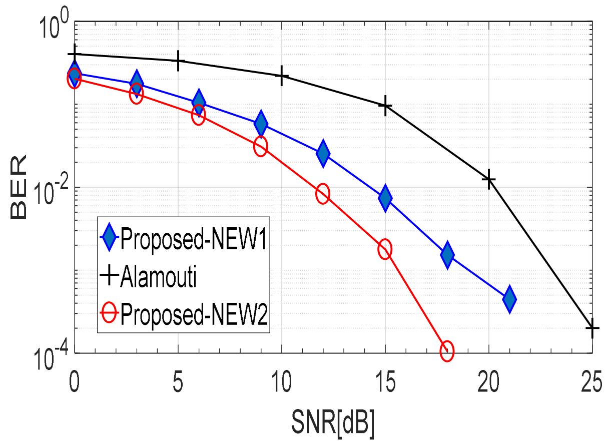

Figure 16. BER performance for the proposed codes and Alamouti code for MN with four distributed antennas

The proposed space-time codes greatly outperform the Alamouti code for the scenario of a master node with four distributed antennas. As can be observed, Proposition 2 achieves a coding gain of more than 9 dB at BER=10^{-3} while Proposition 1 only achieves a gain of roughly 5 dB over the Alamouti code. The graphic demonstrates that under identical environmental conditions, the designed coding parameters of the Proposition 2 space-time code outperform those of the other space-time codes. This is because the MN with four distributed antennas increases the likelihood of line of sight (LoS) and the meticulously designed coding parameters minimize the Euclidean distance. The suggested configuration, in conjunction with the proposed space-time codes, can fulfill the reliability demands, which is BER=10^{-9} for industrial automation for the next generation wireless sensor networks.

VII. CONCLUSIONS

For next-generation wireless sensor networks, two distinct space-time codes are proposed in this research. The Alamouti code is used to compare the proposed codes. The simulation findings demonstrate that a large coding gain can be attained, resulting in more reliable communication to meet the requirements of industrial automation for reliability. The space-time code for Proposition 2 can perform exceptionally well. A setup of master nodes with four distributed antennas is suggested. The combination of the proposed space-time codes and distributed configuration can provide the necessary resilience. This research project has a significant impact on the standardization of the next-generation wireless sensor networks.

References

[1] K. G. Shanthi, S. Sesha Vidhya, G. Vishali, R. V. Uma, M. Thanuja, and S. Srinitha, "Industrial wireless sensor networks with real time data access," *Materials Today: Proceedings*, vol. 80, pp. 2760-2764, 2023. https://doi.org/10.1016/j.matpr.2021.07.033.

[2] W. Liu, and H. Huang, "Design of reliable control software for wireless sensor network testbed," *Proceedings of the Eighth International Conference on Electronic Technology and Information Science (ICETIS 2023)*, SPIE, 2023, vol. 12715, pp. 301-306. https://doi.org/10.1117/12.2682329.

[3] D. Dupleich, N. Han, A. Ebert, R. Müller, S. Ludwig, A. Artemenko, J. Eichinger, T. Geiss, G. Del Galdo, and R. Thomä, "From sub-6 GHz to mm-wave: Simultaneous multi-band characterization of propagation from measurements in industry scenarios," *Proceedings of the 16th IEEE European Conference on Antennas and Propagation (EuCAP)*, 2022, pp. 1-5. https://doi.org/10.23919/EuCAP53622.2022.9768944.

[4] K. Ma, Z. Li, P. Liu, J. Yang, Y. Geng, B. Yang, & X. Guan, "Reliability-constrained throughput optimization of industrial wireless sensor networks with energy harvest in relay," *IEEE Internet of Things Journal*, vol. 8, no. 17, pp.13343-13354, 2021. https://doi.org/10.1109/JIOT.2021.3065966.

[5] L. Liu, G. Han, Z. Xu, L. Shu, M. Martinez-Garcia,, & B. Peng, "Predictive boundary tracking based on motion behavior learning for continuous objects in industrial wireless sensor networks," *IEEE Transactions on Mobile Computing*, vol. 21, no. 9, pp. 3239-3249, 2021. https://doi.org/10.1109/TMC.2021.3049220.

[6] S. Shukla, "Angle based critical nodes detection (ABCND) for reliable industrial wireless sensor networks," *Wireless Personal Communications*, vol. 130, no. 2, pp. 757-775, 2023. https://doi.org/10.1007/s11277-023-10308-4.

[7] S. Gavel, A. S. Raghuvanshi, & S. Tiwari, "A multilevel hybrid anomaly detection scheme for industrial wireless sensor networks," *International Journal of Network Management*, vol. 31, no. 4, pp. 21-44, 2021. https://doi.org/10.1002/nem.2144.

[8] P. Angueira, I. Val, J. Montalban, Ó. Seijo, E. Iradier, P. Sanz Fontaneda, L. Fanari, and A. Arriola, "A survey of physical layer techniques for secure wireless communications in industry," *IEEE Communications Surveys & Tutorials*, vol. 24, no. 2, pp. 810-838, 2022. https://doi.org/10.1109/COMST.2022.3148857.

[9] S. Nandedkar, and S. Nawale, "Frequency and space diverse MIMO antenna with enhanced gain," *Journal of Integrated Science and Technology*, vol. 11, no. 2, pp.482-482, 2023.

[10] D. Mukherjee, K. Gupta, L. H. Chang, and H. Najjaran, "A survey of robot learning strategies for human-robot collaboration in industrial settings," *Robotics and Computer-Integrated Manufacturing*, vol. 73, no. 2, pp. 2231-2240, 2022. https://doi.org/10.1016/j.rcim.2021.102231.

[11] S. Sivakumar, R. Anusuya, V. Nagaraju, L. P. Narendruni, and R. Thamizhamuthu, "QoS based efficient link and consistent routing in wireless sensor network," *Proceedings of the 2023 IEEE International Conference on Intelligent and Innovative Technologies in Computing, Electrical and Electronics (IITCEE)*, 2023, pp. 1241-1246. https://doi.org/10.1109/IITCEE57236.2023.10091080.

[12] W. Zhou, "Research on wireless sensor network access control and load balancing in the industrial digital twin scenario," *Journal of Sensors*, vol. 2022, no. 2, pp. 1-12, 2022. https://doi.org/10.1155/2022/3929958.

[13] Z. Wang, Y. Zhou, A. S. Bajenaid, & Y. Chen, "Design of wireless sensor network using statistical fractal measurements," *Fractals*, vol. 30, no.2, pp. 224-235, 2022. https://doi.org/10.1142/S0218348X22400928.

[14] Z. Li, J. Xie, W. Liu, H. Zhang, and H. Xiang, "Transmit antenna selection and power allocation for joint multi-target localization and discrimination in MIMO radar with distributed antennas under deception jamming," *Remote Sensing*, vol. 14, no. 16, pp. 3904-3920, 2022. https://doi.org/10.3390/rs14163904.

[15] R. Kraemer, M. Methfessel, R. Kays, L. Underberg and A. C. Wolf, "ParSec: A PSSS approach to industrial radio with very low and very flexible cycle timing," *Proceedings of the 2016 24th European Signal Processing Conference (EUSIPCO)*, Budapest, 2016, pp. 1222-1226. https://doi.org/10.1109/EUSIPCO.2016.7760443.

[16] K. Chen-Hu, G. C. Alexandropoulos, and A. G. Armada, "Differential data-aided beam training for RIS-empowered multi-antenna communications," *IEEE Access*, vol.10, no.4, pp. 113200-113213, 2022. https://doi.org/10.1109/ACCESS.2022.3217204.

[17] J. Youn, J. S. Yeom, J. Joung, and B. C. Jung, "Cooperative space-time line code for relay-assisted internet of things," *ICT Express*, vol. 9, no. 2, pp. 253-257, 2023. https://doi.org/10.1016/j.icte.2022.07.004.

[18] I. Dey and N. Marchetti, "Space-Time- and Frequency- Spreading for Interference Minimization in Dense IoT," *IEEE Internet of Things Magazine*, vol. 6, no. 1, pp. 148-153, 2023. https://doi.org/10.1109/IOTM.001.2200174.

[19] A. S. Rajawat, S. B. Goyal, C. Chauhan, P. Bedi, M. Prasad, T. Jan, "Cognitive adaptive systems for industrial internet of things using reinforcement algorithm," *Electronics*, vol. 12, no. 1, pp. 217-226, 2023. https://doi.org/10.3390/electronics12010217.

[20] M. Brachvogel, M. Niestroj, M. Meurer, S. N. Hasnain, R. Stephan, and M. A. Hein, "Space-time adaptive processing as a solution for mitigating interference using spatially-distributed antenna arrays," *Navigation: Journal of the Institute of Navigation*, vol. 70, no. 3, pp. 1-10, 2023. https://doi.org/10.33012/navi.592.

[21] A. Moerman, J. Van Kerrebrouck, O. Caytan, I. Lima de Paula, L. Bogaert, G. Torfs, P. Demeester, H. Rogier, and S. Lemey, "Beyond 5G without obstacles: mmWave-over-fiber distributed antenna systems," *IEEE Communications Magazine*, vol. 60, no. 1, pp. 27-33, 2022. https://doi.org/10.1109/MCOM.001.2100550.

[22] A. Kaplan, J. Vieira, and E. G. Larsson, "Direct link interference suppression for bistatic backscatter communication in distributed MIMO," *IEEE Transactions on Wireless Communications*, vol. 64, no. 2, pp.1-25, 2023. https://doi.org/10.1109/TWC.2023.3285250.

[23] T. Olofsson, A. Ahlén and M. Gidlund, "Modeling of the fading statistics of wireless sensor network channels in industrial environments," *IEEE Transactions on Signal Processing*, vol. 64, no. 12, pp. 3021-3034, 2016. https://doi.org/10.1109/TSP.2016.2539142.

[24] S. Li, J. Zhang and X. Mu, "Non coherent massive space-time block codes for uplink network communications," *IEEE Transactions on Vehicular Technology*, vol. 67, no. 6, pp. 5013-5027, 2018. https://doi.org/10.1109/TVT.2018.2815981.

[25] A. Moerman, J. Van Kerrebrouck, O. Caytan, I. Lima de Paula, L. Bogaert, G. Torfs, P. Demeester, M. Moeneclaey, H. Rogier, and S. Lemey, "mmWave-Over-Fiber distributed antenna systems for reliable multi-Gbps wireless communication," *Proceedings of the 2022 IEEE 3rd URSI Atlantic and Asia Pacific Radio Science Meeting (AT-AP-RASC)*, 2022, pp. 1-4. https://doi.org/10.23919/AT-AP-RASC54737.2022.9814249.

[26] N. A. Kamaruddin, A. Mahmud, M. Y. Bin Alias, A. Abd Aziz, and S. Yaakob, "Performance evaluation of reconfigurable intelligent surface against distributed antenna system at the cell edge," *Electronics*, vol. 11, no. 15, pp. 2376-2388, 2022. https://doi.org/10.3390/electronics11152376.

[27] A. Jabbar, Q. H. Abbasi, N. Anjum, T. Kalsoom, N. Ramzan, S. Ahmed, P. M. Rafi-ul-Shan, O. P. Falade, M. A. Imran, and M. Ur Rehman, "Millimeter-wave smart antenna solutions for URLLC in industry 4.0 and beyond," *Sensors*, vol. 22, no. 7, pp. 2688-2702, 2022. https://doi.org/10.3390/s22072688.

[28] J. Ansari, C. Andersson, P. de Bruin, J. Farkas, L. Grosjean, J. Sachs, J. Torsner et al., "Performance of 5G trials for industrial automation," *Electronics*, vol. 11, no. 3 pp. 412-430, 2022. https://doi.org/10.3390/electronics11030412.

[29] D. Kim, and D.-W. Seo, "Energy-efficient simultaneous wireless information and power transfer-enabled orthogonal multiple access under distributed antenna systems," *Journal of Advanced Marine Engineering and Technology*, vol. 46, no. 4, pp. 196-203, 2022. https://doi.org/10.5916/jamet.2022.46.4.196.

[30] D. Kim, M. Choi, and D.-W. Seo, "Energy-efficient power control for simultaneous wireless information and power transfer–nonorthogonal

multiple access in distributed antenna systems," *IEEE Transactions on Industrial Informatics*, vol. 19, no.7, pp. 8205-8217, 2022. https://doi.org/10.1109/TII.2022.3217503.

[31] S. Jaeckel, L. Raschkowski, K. Borner, L. Thiele, F. Burkhardt, and E. Eberlein, "QuaDRiGa- Quasi Deterministic Radio Channel Generator, user manual and documentation," Fraunhofer Heinrich Herz Institute, Tech. Rep. v1.4.1-551, 2016.

[32] S. Jaeckel, L. Raschkowski, K. Borner, L. Thiele, F. Burkhardt, and E. Eberlein, "QuaDRiGa- Quasi Deterministic Radio Channel Generator, user manual and documentation," Fraunhofer Heinrich Herz Institute, Tech. Rep. v.2.6.1, 2021.

[33] M. El-Absi, S. Galih, M. Hoffmann, M. El-Hadidy and T. Kaiser, "Antenna selection for reliable MIMO-OFDM interference alignment systems: Measurement-based evaluation," *IEEE Transactions on Vehicular Technology*, vol. 65, no. 5, pp. 2965-2977, 2016. https://doi.org/10.1109/TVT.2015.2441133.

[34] A. Mehbodniya, S. Bhatia, A. Mashat, M. Elangovan, and S. Sengan, "Proportional fairness based energy efficient routing in wireless sensor network," *Computer Systems Science & Engineering*, vol. 41, no. 3, pp. 1071-1081, 2022. https://doi.org/10.32604/csse.2022.021529.

[35] S. Mohamed, "A novel robust and low complexity space time codes for industry 4.0 systems," *International Journal of wireless and mobile networks (IJWMN)*, vol. 10, no. 5, pp. 1-16, 2018. https://doi.org/10.5121/ijwmn.2018.10501.

[36] B. Holfeld, et al., "Radio channel characterization at 5.85 GHz for wireless M2M communication of industrial robots," *Proceedings of the 2016 IEEE Wireless Communications and Networking Conference*, Doha, 2016, pp. 1-7. https://doi.org/10.1109/WCNC.2016.7564890.

***MOHAMED S. ABOUZEID** was born in Tanta, Egypt in 1987. He received the B.Sc. (Hons) and M.Sc. degrees in Electrical communication engineering from Tanta University, Tanta, Egypt in 2009 and 2014, respectively. From 2010 to 2014, Abouzeid was a Research Assistant with Faculty of Engineering, Tanta University. From 2014 till now, Abouzeid has worked as Assistant Lecturer in Electronics and Electrical Communication Department at Faculty of Engineering, Tanta University. Abouzeid works in several research projects focusing on 5G mobile technologies. His research interests include massive MIMO, RFID, Distributed Antenna Systems, Localization and other potential 6G technologies.*

***HEBA A. EL-KHOBBY** received the B.Sc.(Hons), MSc and Ph.D. degrees, from Tanta University, Tanta, Egypt, Faculty of Engineering, in 1998, 2003, and 2009 respectively. Since 2009, she has been a Teaching Staff Member with the Department of Electronics and Electrical Communications Engineering, Faculty of Engineering, Tanta University. Her current research interests include image enhancement, image restoration, image interpolation, super-resolution reconstruction of images, medical image processing, data hiding, multimedia communications, and wireless communications.*

***MAHMOUD A. A. ALI** received his Ph.D. in Wireless Communications Engineering from Monoufiya University, Egypt in 1991 and his M.Sc. in Wireless Communications Engineering from Monoufiya University in 1987 and B.Sc. (Hons) in Electrical communication engineering from Monoufiya University in 1979. He is currently a professor of Wireless Communications in Tanta University. He was the head of Electronics and Electrical Communications department in Faculty of Engineering, Tanta University from 2015 to 2017.*

***MOHAMED E. NASR** received his Ph.D. in Digital Communications Engineering from Delhi University in 1985 and his M.Sc. in Electrical Communications Engineering from Mansoura University in 1979 and B.Sc. (Hons) in Computer Engineering from Monoufiya University, Egypt in 1975. He is currently a professor of Wireless Communications in Tanta University. He was the head of Electronics and Electrical Communications department in Faculty of Engineering, Tanta University from 2004 to 2008.*